Supplement of Earth Syst. Dynam., 7, 559–582, 2016
http://www.earth-syst-dynam.net/7/559/2016/
doi:10.5194/esd-7-559-2016-supplement

Supplement of

Climate change increases riverine carbon outgassing, while export to the ocean remains uncertain

F. Langerwisch et al.

Correspondence to: F. Langerwisch (langerwisch@pik-potsdam.de)

1 Respiration of litter and soil carbon

The respiration of the un-respired litter carbon and the soil carbon has been calculated analogous to the LPJmL functions with Eqs. (S1) to (S12)

$$Litc_{unresp_{loss}} = Litc_{unresp_t} \times (1 - e^{-(respi_{litc} \times Tresponse_t)}) \tag{S1}$$

$$Litc_{loss} = Litc_t \times (1 - e^{-(respi_{litc} \times Tresponse_t)}) \tag{S2}$$

$$lrLitc_{unresp_t} = Litc_{unresp_t} - Litc_{unresp_{loss}} \tag{S3}$$

$$lrLitc_t = Litc_t - Litc_{loss} \tag{S4}$$

$$Litc_t = lrLitc_t + lrLitc_{unresp_t} \tag{S5}$$

$$lrSoilc_{fast_t} = Soilc_{fast_t} + respipart_{soilcfast}(Litc_{unresp_{loss}} + Litc_{unresp_{loss}}) \tag{S6}$$

$$lrSoilc_{slow_t} = Soilc_{slow_t} + respipart_{soilcslow}(Litc_{unresp_{loss}} + Litc_{unresp_{loss}}) \tag{S7}$$

$$Soilc_{fast_{loss}} = lrSoilc_{fast_t} \times (1 - e^{-(respi_{soilfast} \times Tresponse_t)}) \tag{S8}$$

$$Soilc_{slow_{loss}} = lrSoilc_{slow_t} \times (1 - e^{-(respi_{soilslow} \times Tresponse_t)}) \tag{S9}$$

$$srSoilc_{fast_t} = lrSoilc_{fast_t} - srSoilc_{fast_{loss}} \tag{S10}$$

$$srSoilc_{slow_t} = lrSoilc_{slow_t} - srSoilc_{slow_{loss}} \tag{S11}$$

$$Soilc_t = srSoilc_{fast_t} + srSoilc_{slow_t} \tag{S12}$$

with $respipart_{soilcfast}$ being the fraction of litter that enters the soil organic carbon pool with fast respiration and $respipart_{soilslow}$ being the fraction of litter that enters the soil organic carbon pool with slow respiration.

2 Mobilization

The mobilization takes place in the cell heterogeneously. It occurs first closest to the river. The cells are therefore divided into fractions, which size depends on the vicinity to the river, with section 6 closest to the river.

Figure S1: Depiction of the fraction of each cell section.

3 Sensitivity analysis

3.1 Initial parameter setting and quality

The parameterization of the model builds upon an analysis of the scientific literature. The parameters used within the model originate from a number of sources and are of differing quality. Table S1 lists all parameters and their sources. In addition to the parameter value, it also provides the value ranges and a first quality assessment of the parameter values based on the methods used in the relevant studies. The quality was weighted medium to low if the measurements took place in a slightly other system, for instance in the *Igapó* instead of *Várzea*, or are only based on one single observation. The quality and the relevance of single parameters for the simulation outputs are further tested in the sensitivity analysis.

Table S1: Initial parameter setting. List of parameters and parameter quality (high, medium, low).

parameter name	*initial value*	*unit*	*source*	*quality*
mobilization				
carboncorr	0.65 ± 0.15	month^{-1}	(Worbes, 1997)	high
$mobil_{litc}$	0.4 ± 0.1	month^{-1}	(Irmler, 1982)	medium
$mobil_{soilc}$	0.008 ± 0.002	month^{-1}	(Irmler, 1982)	low
$mobil_{p}$	0.5 ± 0.25	-	(McClain and Elsenbeer, 2001; Johnson et al., 2006)	medium
decomposition				
decomp	0.3 ± 0.1	month^{-1}	(Furch and Junk, 1997)	high
decompcorr	0.1 ± 0.01	month^{-1}	(Furch and Junk, 1997)	high
respiration				
respi	0.045 ± 0.01	day^{-1}	(Cole et al., 2000)	high
outgassing				
co2satur	7.25 to 17.0	-	(Richey et al., 2002)	high

3.2 Simulations for sensitivity analysis

The model RivCM has been run on a 0.5° × 0.5° spatial resolution for the period 1901-2003. The transient runs have been preceded by a 90-years-spinup during which the climate, CO_2 levels and carbon input (litter and soil) of 1901-1930 have been repeated to obtain equilibrium for the riverine carbon pools. As input to the terrestrial litter and soil carbon pools, LPJmL results produced under the CRU TS2.1 climate (Österle et al., 2003; Mitchell and Jones, 2005) has been used. The transient LPJmL runs have been preceded by a 1,000-years-spinup during which the pre-industrial CO_2 level of 280 ppm and the climate of the years 1901-1930 have been repeated to obtain equilibrium for vegetation, carbon and, water pools. For this analysis, simulations have been conducted with an initial parameter setting (see Table S1) and a modified parameter setting (Table S2).

Table S2: List of parameters modified for the sensitivity analysis. All parameters have been multiplied with the following factors: 0.1; 0.5; 0.9; 1.1; 1.5; 1.9.

parameter name	*original value*	*modified value*
mobilization		
$mobil_{litc}$	0.4	0.04; 0.2; 0.36; 0.44; 0.6; 0.76
$mobil_{soilc}$	0.008	0.0008; 0.004; 0.0072; 0.0088; 0.012; 0.0152
$mobil_{p}$	0.5	0.05; 0.25; 0.45; 0.55; 0.75; 0.95
decomposition		
decomp	0.3	0.03; 0.15; 0.27; 0.33; 0.45; 0.57
respiration		
respi	0.045	0.0045; 0.0225; 0.0405; 0.0495; 0.0675; 0.0855

The sensitivity analysis aims to estimate the effect of changes in the explaining variables on the response variables. The results of these simulations have been analysed with a redundancy analysis (RDA). This analysis is, comparable to PCA, an ordination technique which identifies the most important separator of a given dataset (including all response variables) and also the most important initiator (explaining variables) of dataset's variability. The sensitivity analysis led to a partly adapted parameter setting (standard parameters). For evaluation, simulations under the standard parameter setting (see Table 3 row ‘original value’) have been conducted. The results of these simulations have been compared to several observed values (Table 4).

3.3 Results of sensitivity analysis

The aim of a sensitivity analysis is to estimate which output variable (response variable) is most sensitive to changing parameters (explaining variables), and which parameter changes cause the larges shifts in the output values.

To analyse the results of the simulation of the sensitivity analysis a redundancy analysis (RDA) has been performed. The results of the redundancy analysis (for parameters see Table S2) are summarized in and Table S3. This analysis shows the effect of the explaining variables, i.e. parameters, $mobil_{litc}$, $mobil_{soilc}$, $mobil_{p}$, *decomp* and *respi* on the response variables riverine particulate organic carbon (POC), riverine dissolved organic carbon (DOC), riverine inorganic carbon (IC) and outgassed carbon. The parameter changes did not cause changes in IC, since it is only temperature and atmospheric CO_2 dependent. Therefore, IC has not been included in this analysis.

The RDA shows that 79.2% of the variance within the dataset can be described by the explaining variables (therefore, 20.8% cannot be explained by explaining variables).

The first, second, and third axis explain 54%, 18.9%, and 6.3% of the variance within the dataset, respectively. The variance of the response variables TOC concentration, DOC concentration, and POC concentration are mainly influenced by the first axis (RDA1) with loadings (*prop*) of −0.23, −0.21, and −0.18, respectively (depicted in red in Figure S2, listed in Table S3). This axis is primarily controlled by *respi* (0.79) and $mobil_{litc}$ (−0.59) (blue arrows in Figure S2). The variance of the response variable outgassed CO_2 is mainly influenced by RDA2 with a loading of −0.075. This axis is also primarily controlled by *respi* (−0.60) and $mobil_{litc}$ (−0.78), but in a swapped order and, in contradiction to RDA1, not in opposite directions. The third axis (RDA3) mainly influences the response variables POC concentration and DOC concentration, with loadings of 0.013 and −0.008, respectively. This axis is primarily controlled by $mobil_{p}$ (0.81) and *decomp* (−0.59).

Therefore, the parameters that explain most of the variance within the dataset are *respi* and $mobil_{litc}$. The parameters $mobil_{p}$ and *decomp* have only little effect on the variance of the whole dataset. The most and nearly equally influenced output variables are TOC concentration and DOC concentration. POC concentration and outgassed CO_2 are only marginally affected.

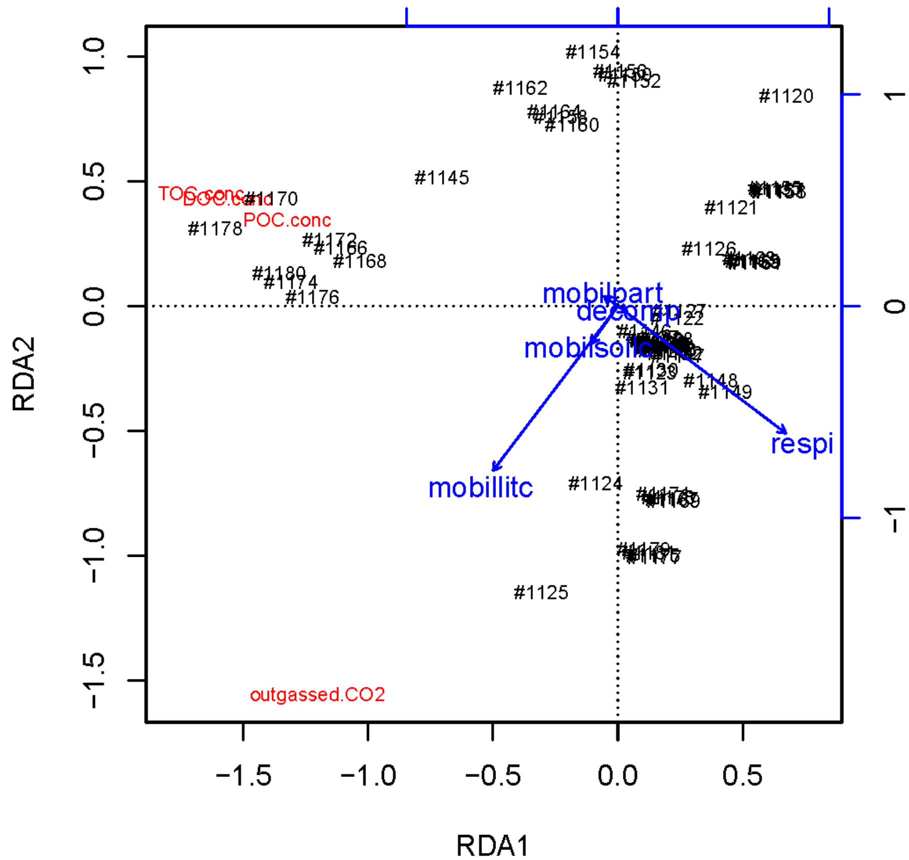

Figure S2: Results of the redundancy analysis. Redundancy analysis with all simulations associated with the sensitivity analysis (black numbers). The four output variables (red) have been calculated with five parameters (blue).

Table S3: Results of the redundancy analysis. Results for the first three RDA axes. Original value per axis (*axis*) and values proportional to the explained variability of the whole dataset (*prop*) with a general scaling constant of species scores of Cs = 3.9523.

	RDA1		*RDA2*		*RDA3*	
Proportion explained						
	0.540		0.189		0.063	
Species scores (response variables)						
	axis	*prop*	*axis*	*prop*	*axis*	*prop*
TOC concentration	−1.668	−0.228	0.4523	0.0216	−0.1601	−0.0026
POC concentration	−1.325	−0.181	0.3446	0.0165	0.8283	0.0132
DOC concentration	−1.564	−0.214	0.4296	0.0205	−0.5249	−0.0084
outgassed CO_2	−1.204	−0.164	−1.5634	−0.0748	−0.0080	−0.0001
Variable scores (explaining variables)						
	axis	*prop*	*axis*	*prop*	*axis*	*prop*
$mobil_{litc}$	−0.5900	−0.3185	−0.77757	−0.14696	−0.00312	−0.00020
$mobil_{soilc}$	−0.1262	−0.0681	−0.17715	−0.03348	−0.00110	−0.00007
$mobil_p$	−0.0650	−0.0351	0.04598	0.00869	0.80759	0.05104
decomp	0.0452	0.0244	−0.03163	−0.00598	−0.58934	−0.03725
respi	0.7941	0.4287	−0.60111	−0.11361	0.08909	0.00563

4 Calibration and validation

As a result of the sensitivity analysis, we calibrated values of the most important explaining variables (parameters) $mobil_{litc}$, $mobil_{soilc}$ and *respi* (Tables 3 and 4). After calibration the Willmott's Index of Agreement, with 1 indicating complete agreement between observation and simulation results (Willmott, 1982), is 0.615, compared to 0.427 with the initial parameter values (Table 4). The calibrated rate of respiration (*respi)* lies within the observed range, while the two other calibrated parameters ($mobil_{litc}$, $mobil_{soilc}$) are larger than observed values by a factor of 1.4 and 5, respectively (Table 3). However, the observations available were only conducted in a *Várzea* ecosystem and $mobil_{soilc}$ and are only estimated.

Spatial pattern and distribution of the carbon pools as calculated with the standard parameter setting are shown in Figure 4. The two organic carbon pools POC and DOC show the same spatial pattern with high amounts concentrated along the river, and only differ in the actual values with POC displaying half the amount of DOC (max. 0.2×10^{8} g km^{-2} vs. max. 0.4×10^{8} g km^{-2}, Fig. S3). In contrast, the two inorganic carbon pools differ in their spatial pattern. The amount of inorganic carbon per cell (IC) increased up to 0.25×10^{8} g km^{-2} with increasing river discharge. The outgassed carbon is more homogeneously distributed in the catchment. Here, also the river network in combination with the floodplain can be identified. Therefore, the pattern is less pronounced than in the other carbon pools.

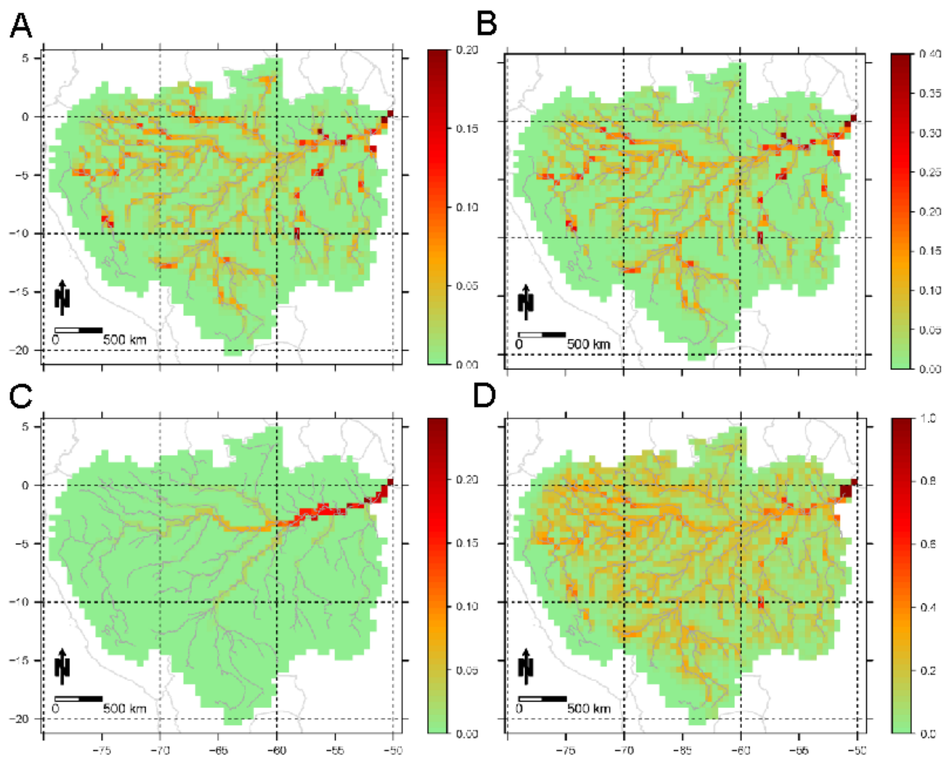

Figure S3: Spatial distribution of the four carbon species used in the further analysis. (A) Riverine particulate organic carbon (POC), (B) dissolved organic carbon (DOC), (C) inorganic carbon (IC) and (D) outgassed carbon [10^{8} g km^{-2}] in 2003 obtained from simulations forced by CRU TS2.1.

5 Additional maps showing similar patterns for POC and DOC

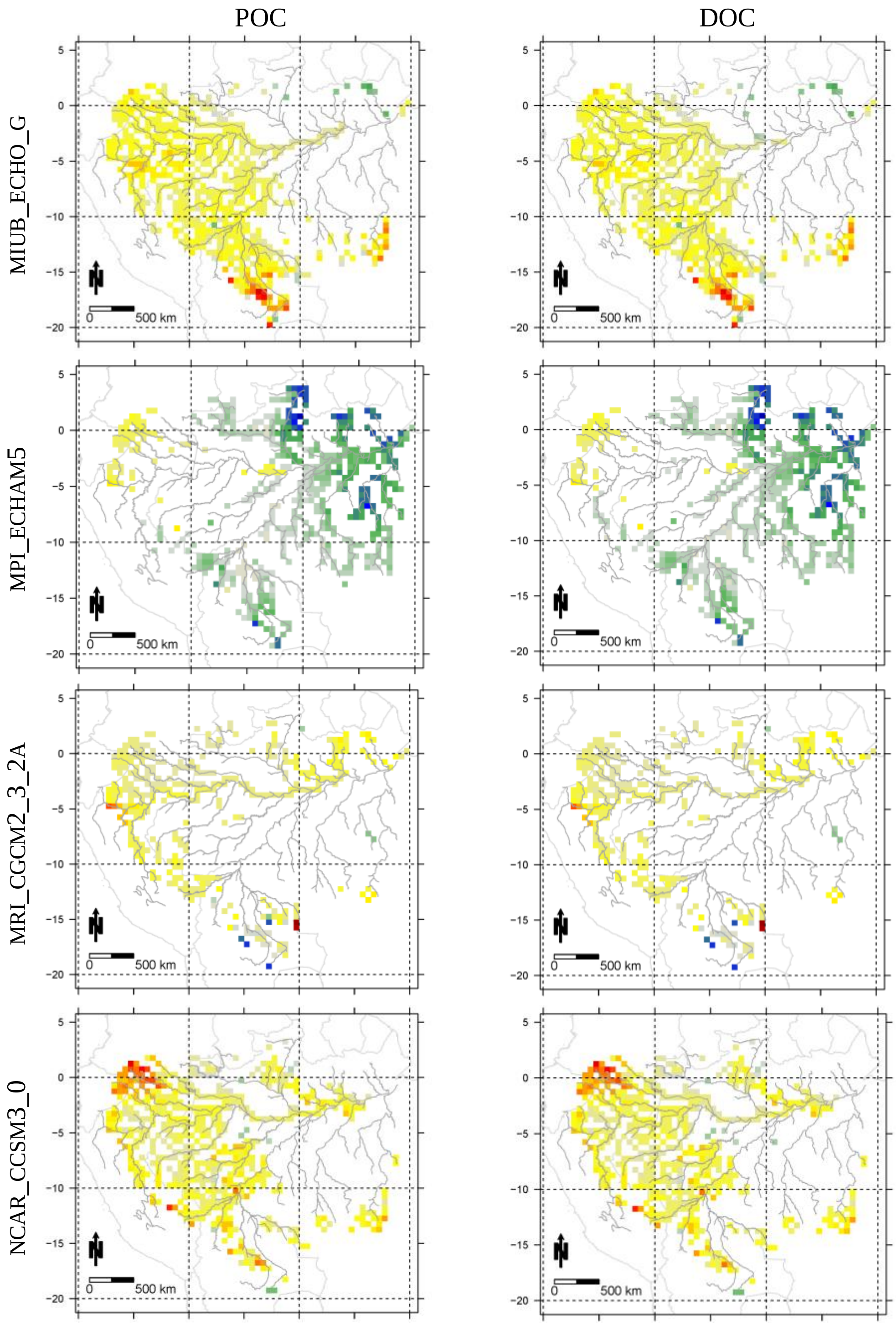

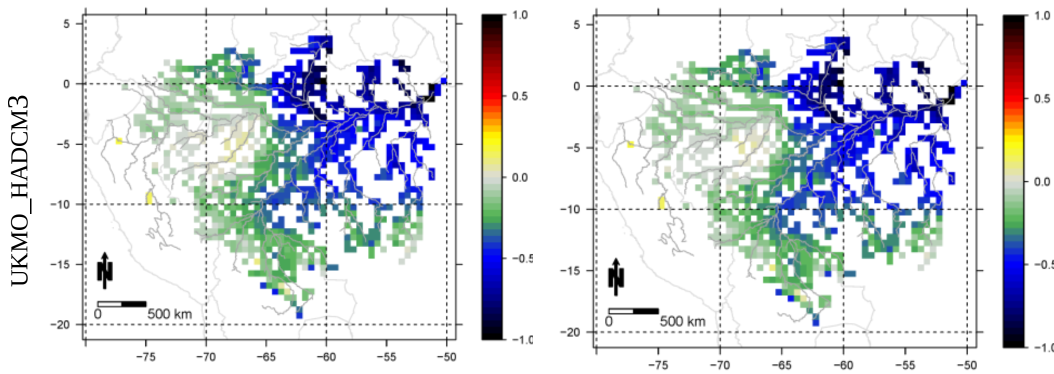

Figure S4: Changes in particulate organic carbon (POC) and dissolved organic carbon (DOC) caused by climate change. Quotient (log10) of mean future and mean reference carbon amount for each climate model/scenario under emission scenario A1B. Positive values indicate an increase and negative values indicate decrease.

6 References

Belger, L., Forsberg, B. R. and Melack, J. M.: Carbon dioxide and methane emissions from interfluvial wetlands in the upper Negro River basin, Brazil, Biogeochemistry, 105, 171–183, doi:10.1007/s10533-010-9536-0, 2011.

Cole, J. J., Pace, M. L., Carpenter, S. R. and Kitchell, J. F.: Persistence of net heterotrophy in lakes during nutrient addition and food web manipulations, Limnol. Oceanogr., 45(8), 1718–1730, 2000.

Devol, A. H., Quay, P. D., Richey, J. E. and Martinelli, L. A.: The role of gas-rxchange in the inorganic carbon, oxygen, and Rn-222 budgets of the Amazon river, Limnology and Oceanography, 32(1), 235–248, 1987.

Furch, K. and Junk, W. J.: The chemical composition, food value, and decomposition of herbaceous plants, leaves, and leaf litter of floodplain forests, in The Central Amazon Floodplain, edited by W. J. Junk, pp. 187–205, Springer, Berlin, Germany., 1997.

Irmler, U.: Litterfall and nitrogen turnover in an Amazonian blackwater inundation forest, Plant and Soil, 67(1-3), 355–358, 1982.

Johnson, M. S., Lehmann, J., Selva, E. C., Abdo, M., Riha, S. and Couto, E. G.: Organic carbon fluxes within and streamwater exports from headwater catchments in the southern Amazon, Hydrological Processes, 20(12), 2599–2614, 2006.

Junk, W. J. and Wantzen, K. M.: The flood pulse concept: New aspects, approaches and applications - An update, in Proceedings of the Second International Symposium on the Management of large Rivers for Fisheries, edited by R. L. Welcomme and T. Petr, pp. 117–140., 2004.

Lewin-Koh, N. J. and Bivand, R.: maptools: Tools for reading and handling spatial objects. R package version 0.8-7., 2011.

McClain, M. E. and Elsenbeer, H.: Terrestrial inputs to Amazon streams and internal biogeochemical processing, in The Biogeochemistry of the Amazon Basin, edited by M. E. McClain, R. L. Victoria, and J. E. Richey, pp. 185–208, Oxford University Press, New York., 2001.

Melack, J. M. and Forsberg, B.: Biogeochemistry of Amazon floodplain lakes and associated wetlands, in The Biogeochemistry of the Amazon Basin and its Role in a Changing World, pp. 235–276, Oxford University Press, Eds. McClain, M. E.; Victoria, R. L.; Richey, J. E., 2001.

Neu, V., Neill, C. and Krusche, A. V.: Gaseous and fluvial carbon export from an Amazon forest watershed, Biogeochemistry, 105, 133–147, doi:10.1007/s10533-011-9581-3, 2011.

Oksanen, J., Blanchet, F. G., Kindt, R., Legendre, P., O'Hara, R. B., Simpson, G. L., Solymos, P., Stevens, M. H. H. and Wagner, H.: vegan: Community Ecolgy Package. R package version 1.17.11. [online] Available from: http://CRAN.R-project.org/package=vegan, 2011.

Poulter, B., Aragão, L., Heyder, U., Gumpenberger, M., Heinke, J., Langerwisch, F., Rammig, A., Thonicke, K. and Cramer, W.: Net biome production of the Amazon Basin in the 21st century, Global Change Biology, 16(7), 2062–2075, doi:10.1111/j.1365-2486.2009.02064.x, 2009.

Rammig, A., Jupp, T., Thonicke, K., Tietjen, B., Heinke, J., Ostberg, S., Lucht, W., Cramer, W. and Cox, P.: Estimating the risk of Amazonian forest dieback, New Phytologist, 187(3), 694–706, doi:10.1111/j.1469-8137.2010.03318.x, 2010.

R Development Core Team and contributors worldwide, N. J.: stats: The R Stats Package version 2.13.0., 2011.

Richey, J. E., Melack, J. M., Aufdenkampe, A. K., Ballester, V. M. and Hess, L. L.: Outgassing from Amazonian rivers and wetlands as a large tropical source of atmospheric CO_2, Nature, 416(6881), 617–620, doi:10.1038/416617a, 2002.

Silva, T. S. F., Costa, M. P. F. and Melack, J. M.: Annual net primary production of macrophytes in the Eastern Amazon floodplain, Wetlands, 29(2), 747–758, 2009.

Sippel, S. J., Hamilton, S. K. and Melack, J. M.: Inundation area and morphometry of lakes on the Amazon River floodplain, Brazil, Archiv Fuer Hydrobiologie, 123(4), 385–400, 1992.

Willmott, C. J.: Some comments on the evaluation of model performance, Bulletin American Meteorological Society, 63(11), 1309–1313, 1982.

Worbes, M.: The forest ecosystem of the floodplains, in The Central Amazon Floodplain, edited by W. J. Junk, pp. 223–265, Springer, Berlin, Germany., 1997.